

# Inclusive Diffraction at HERA

F.-P. Schilling<sup>a\*</sup> (on behalf of the H1 and ZEUS collaborations)

<sup>a</sup>DESY, Notkestr. 85, D-22603 Hamburg, Germany

New precision measurements of inclusive diffractive deep-inelastic  $ep$  scattering interactions, performed by the H1 and ZEUS collaborations at the HERA collider, are discussed. A new set of diffractive parton distributions, determined from recent high precision H1 data, is presented.

## 1. INTRODUCTION

One of the biggest challenges in our understanding of QCD is the nature of colour singlet exchange or *diffractive* interactions. The electron-proton collider HERA is an ideal place to study hard diffractive processes in deep-inelastic  $ep$  scattering (DIS). In such interactions, the point-like virtual photon probes the structure of colour singlet exchange, similarly to inclusive DIS probing proton structure.

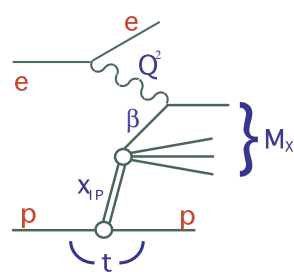


Figure 1: Illustration of a diffractive DIS event.

a large rapidity gap without particle production between the central hadronic system and the proton beam direction.

A diagram of diffractive DIS is shown in Fig. 1. A virtual photon coupling to the beam electron interacts diffractively with the proton through the exchange of a colour singlet and produces a

At HERA, around 10% of low  $x$  events are diffractive [1]. Experimentally, such events are identified by either tagging the elastically scattered proton in *Roman pot* spectrometers 60–100 m downstream from the interaction point or by asking for

hadronic system  $X$  with mass  $M_X$  in the final state. If the 4-momenta of the incoming (outgoing) electron and proton are labeled  $l$  ( $l'$ ) and  $p$  ( $p'$ ) respectively, the following kinematic variables can be defined:  $Q^2 = -q^2 = -(l - l')^2$ , the photon virtuality;  $\beta = Q^2/q \cdot (p - p')$ , the longitudinal momentum fraction of the struck quark relative to the diffractive exchange;  $x_{\mathbb{P}} = q \cdot (p - p')/q \cdot p$ , the fractional proton momentum taken by the diffractive exchange and  $t = (p - p')^2$ , the 4-momentum squared transferred at the proton vertex. Bjorken- $x$  is given by  $x = x_{\mathbb{P}}\beta$ . For the measurements presented here typical values of  $x_{\mathbb{P}}$  are  $< 0.05$ .  $y = Q^2/sx$  denotes the inelasticity, where  $s$  is the  $ep$  CMS energy.

A diffractive *reduced cross section*  $\sigma_r^{D(4)}$  can be defined via

$$\frac{d^4\sigma^{ep \rightarrow eXp}}{dx_{\mathbb{P}} dt d\beta dQ^2} = \frac{4\pi\alpha^2}{\beta Q^4} \left(1 - y + \frac{y^2}{2}\right) \sigma_r^{D(4)}(x_{\mathbb{P}}, t, \beta, Q^2), \quad (1)$$

which is related to the diffractive structure functions  $F_2^D$  and the longitudinal  $F_L^D$  by

$$\sigma_r^D = F_2^D - \frac{y^2}{2(1 - y + \frac{y^2}{2})} F_L^D. \quad (2)$$

Except at the highest  $y$ ,  $\sigma_r^D = F_2^D$  to a very good approximation. If the outgoing proton is not detected, the measurements are integrated over  $t$ :  $\sigma_r^{D(3)} = \int dt \sigma_r^{D(4)}$ .

\*e-mail address: fpschill@mail.desy.de

## 2. FACTORIZATION PROPERTIES OF DIFFRACTIVE DIS

The proof [2] that QCD hard scattering factorization is valid for diffractive DIS justifies the expression of  $\sigma_r^{D(4)}$ , at fixed  $x_P$  and  $t$ , as a convolution of diffractive proton parton distributions (dpdf's)  $f_i^D$  and partonic cross sections  $\hat{\sigma}^{\gamma^*i}$ :

$$\sigma_r^{D(4)} \sim \sum_i \hat{\sigma}^{\gamma^*i}(x, Q^2) \otimes f_i^D(x, Q^2, x_P, t). \quad (3)$$

The  $f_i^D$  should obey the DGLAP evolution equations and the  $\hat{\sigma}^{\gamma^*i}$  are the same as for standard DIS. In consequence, the framework of NLO QCD can be applied to diffractive DIS in a similar way as to inclusive DIS.

An extra assumption which is often made is that the  $(x_P, t)$  dependence of  $\sigma_r^D$  can be factored out (Regge factorization) into a *Pomeron flux factor*  $f_P(x_P, t)$ :

$$f_i^D(x_P, t, \beta, Q^2) = f_P(x_P, t) f_i^P(\beta, Q^2), \quad (4)$$

which is often parameterised using Regge phenomenology as

$$f_P(x_P, t) = x_P^{1-2\alpha_P(t)} e^{bt}, \quad (5)$$

where  $\alpha_P(t) = \alpha_P(0) + \alpha'_P t$  is the pomeron trajectory with intercept  $\alpha_P(0)$ . The  $f_i^P(\beta, Q^2)$  are *Pomeron pdf's*. Although there is no firm basis in QCD for Eq. 4, it is approximately consistent with present data.

## 3. EXPERIMENTAL RESULTS

### 3.1. The New Datasets

The H1 collaboration has performed several new measurements of diffractive DIS, presented in the form of the reduced cross section  $\sigma_r^{D(3)}$ , which are summarised in Fig. 2. Two high precision measurements in the kinematic range  $1.5 < Q^2 < 120 \text{ GeV}^2$  (labeled 'H1 99' [3] and 'H1 97' [4]) are based on the rapidity gap method. With respect to previous H1 data [5], a factor of typically 5 more data were analysed and the kinematic range was extended significantly to lower  $Q^2$  and  $\beta$ . Another new measurement using a forward proton spectrometer covers  $2.5 < Q^2 < 20 \text{ GeV}^2$  ('H1 99-00 FPS', [6]). Good agreement between the

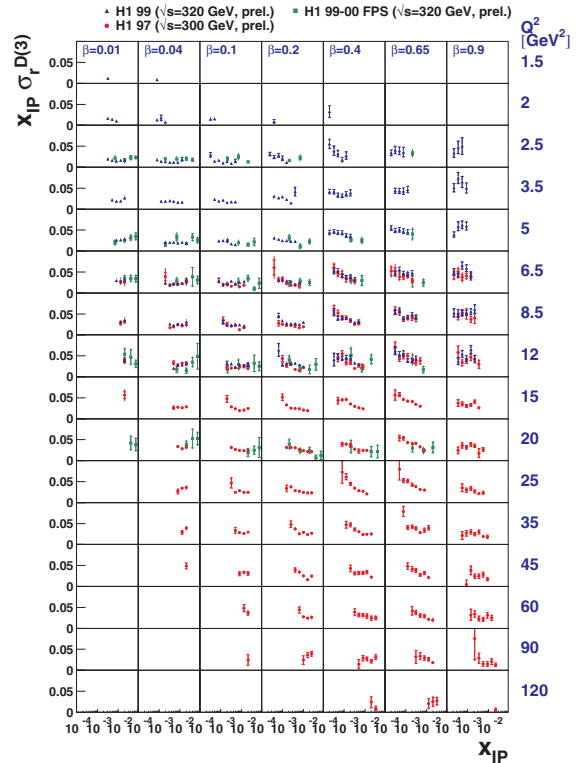


Figure 2. Compilation of new measurements of the diffractive reduced cross section  $\sigma_r^D$  by H1.

different data sets and measurement techniques is observed.

The ZEUS collaboration has presented new data [7] on  $F_2^{D(3)}$  for  $2.2 < Q^2 < 80 \text{ GeV}^2$ , shown in Fig. 3. Diffractive events are selected by reconstructing a low value of  $M_X$  in the detector. The data correspond to a factor 2 increase in integrated luminosity with respect to previous results [8]. ZEUS has also measured (Fig. 4, [9]) the diffractive cross section in the transition region  $0.03 < Q^2 < 0.6 \text{ GeV}^2$  between DIS and quasi-real photon-proton interactions ( $Q^2 \sim 0$ ). Also shown in Fig. 4 is a fit based on a dipole model [10] in which the photon fluctuates into  $q\bar{q}$  and  $q\bar{q}g$  states.

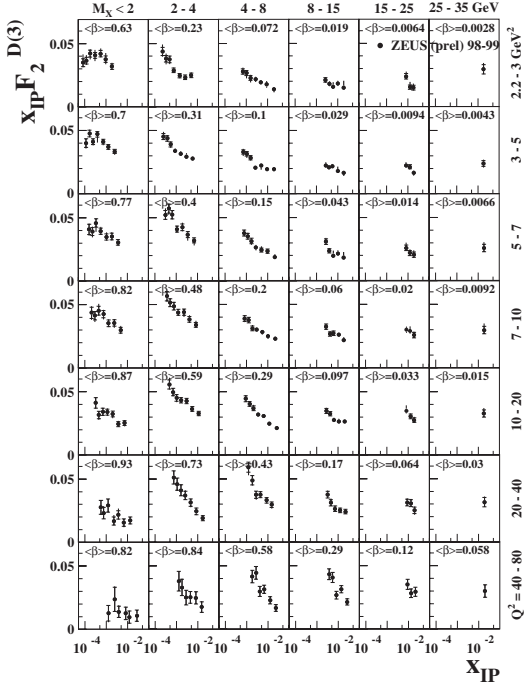


Figure 3. New measurement of the structure function  $F_2^{D(3)}$  by ZEUS.

### 3.2. $t$ and $\Phi_{ep}$ Dependences

Both collaborations have measured the  $t$  dependence of the cross section using their forward proton spectrometers. In the measured range  $-0.45 \lesssim t < -|t|_{min}$ , an exponential dependence  $\frac{d\sigma}{dt} \sim e^{bt}$  is observed and the slope parameter  $b$  is determined for different values of  $x_P$  (Fig. 5). Models based on Regge phenomenology predict an increasing steepness of the  $t$  dependence with energy (*shrinkage*):  $b = b_0 + 2\alpha' \log \frac{1}{x_P}$ . As can be seen in Fig. 5, the data at low  $x_P$  are so far inconclusive.

ZEUS has studied [11] the cross section dependence on the azimuthal angle  $\Phi_{ep}$  between the electron and proton scattering planes, which is sensitive to the longitudinal cross section  $\sigma_L^D$  via the interference between transverse and longitudinal photon induced contributions, which introduces an asymmetry in  $\Phi_{ep}$ . The measured asymmetries are small and, within the present statistical uncertainties, compatible with zero.

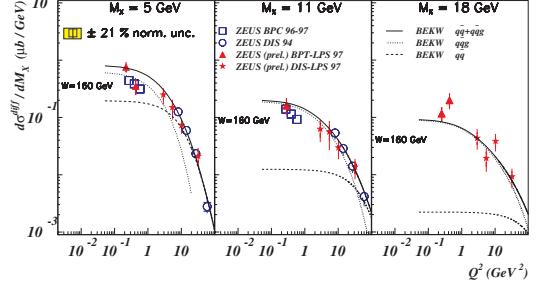


Figure 4. New measurement of the diffractive cross section at low  $Q^2$  by ZEUS.

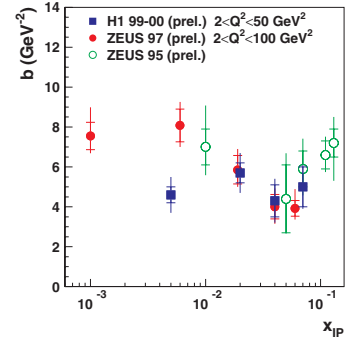


Figure 5. The slope parameter  $b$  from fits to  $\frac{d\sigma}{dt} \sim e^{bt}$  at different values of  $x_P$ .

### 3.3. $x_P$ Dependence

By making fits to the  $x_P$  dependence of the diffractive DIS data using Eqs. 4,5, values for the effective pomeron intercept  $\alpha_P(0)$  are determined. Results for measurements at different  $Q^2$  are shown in Fig. 6 and compared with the *soft pomeron* value of 1.08 as well as with a parameterisation based on inclusive DIS data, obtained from fits of the form  $F_2(x, Q^2) \sim cx^{-\lambda(Q^2)}$  where  $\lambda = \alpha_P(0) - 1$ . The diffractive data suggest an increase of  $\alpha_P(0)$  with  $Q^2$  and are significantly higher than the soft pomeron value for  $Q^2 \gtrsim 10$  GeV. However, the naive expectation that the diffractive cross section grows twice as fast with energy as the inclusive one, correspond-

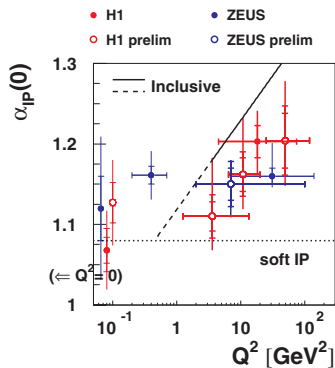


Figure 6. Measurements of the effective pomeron intercept  $\alpha_{\mathcal{P}}(0)$  for different values of  $Q^2$ , compared with a parameterisation from inclusive DIS.

ing to  $\alpha_{\mathcal{P}}^{dif.}(0) = \alpha_{\mathcal{P}}^{incl.}(0)$ , is hard to reconcile with the present data at high  $Q^2$ .

### 3.4. Ratio of Diffractive to Inclusive Cross Section

H1 has studied [4] the logarithmic  $Q^2$  dependence of the ratio of the diffractive to the inclusive DIS reduced cross sections, presented as the quantity  $f_{\mathcal{P}}(x_{\mathcal{P}})^{-1} d/d\ln Q^2(\sigma_r^D/\sigma_r)$  in Fig. 7 for different  $\beta$  and  $x_{\mathcal{P}}$  values. Taking out the factorising  $x_{\mathcal{P}}$  dependence, the same behaviour is observed at different  $x_{\mathcal{P}}$ : At low  $\beta$ , the logarithmic  $Q^2$  dependences of  $\sigma_r^D$  and  $\sigma_r$  are very similar, indicating that the ratio of the diffractive to the total proton gluon density is approximately constant in this region. By contrast, at the highest  $\beta \gtrsim 0.5$ , the logarithmic  $Q^2$  derivative becomes negative, suggestive of the presence of  $Q^2$ -suppressed higher twist contributions to  $\sigma_r^D$  for  $\beta \rightarrow 1$ . However, this behaviour can also be explained by DGLAP evolution due to the kinematic limit  $x = x_{\mathcal{P}}$  ( $\beta = 1$ ) for gluon radiation in the case of  $\sigma_r^D$ .

## 4. $\beta$ AND $Q^2$ DEPENDENCES OF $\sigma_r^D$ AND NLO QCD FIT TO H1 DATA

H1 has presented [4] a new NLO DGLAP QCD fit to the diffractive reduced cross section data,

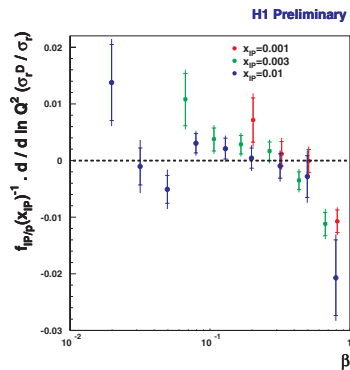


Figure 7. Logarithmic  $Q^2$  derivatives of the ratio  $\sigma_r^D/\sigma_r$  from H1, divided by  $f_{\mathcal{P}}(x_{\mathcal{P}})$ , shown as a function of  $\beta$  for different  $x_{\mathcal{P}}$ .

from which diffractive parton densities are determined. The shape of the dpdf's is assumed to be independent of  $x_{\mathcal{P}}$  (Regge factorization), in agreement with the data, as can be seen in Figs. 8 and 9. The precisely measured  $\beta$  and  $Q^2$  dependences of the data are compared with the fit result, dividing out the  $x_{\mathcal{P}}$  dependence, parameterised as stated in Eq. 5.

The diffractive exchange is parameterised by a light flavour singlet and a gluon distribution at a starting scale  $Q_0^2 = 3 \text{ GeV}^2$  and evolved to higher  $Q^2$  using the standard NLO DGLAP equations. For the first time in diffraction, the experimental and model uncertainties are propagated to obtain error bands for the dpdf's.

The result of the fit is presented in Fig. 10. The diffractive pdf's remain large up to large fractional momenta  $z$  (or  $\beta$ ) and are dominated by the gluon distribution. In total 75% of the exchange momentum is carried by gluons at  $Q^2 = 10 \text{ GeV}^2$ . To test factorization, the dpdf's can be used for updated comparisons with diffractive final state data from HERA and the TEVATRON [4,12].

## 5. CONCLUSIONS

Several new high precision data sets of inclusive diffractive DIS have recently become available. In the case of the rapidity gap method, the data are

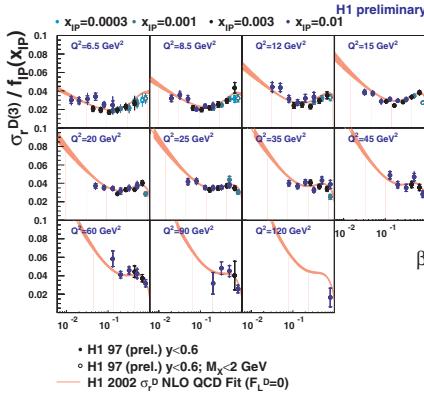


Figure 8.  $\beta$  dependence of  $\sigma_r^D$  from H1, scaled by  $f_P(x_P)^{-1}$  and compared with the NLO QCD fit.

now systematically limited at low  $Q^2$ . These data are very useful to constrain the free parameters of QCD motivated models (e.g. dipole models) for diffractive DIS and to distinguish between different approaches. In particular, they have been used for the determination of a new generation of diffractive parton distributions – including their uncertainties – in the framework of NLO QCD, enabling tests of QCD factorization as applied to diffraction by comparisons with final state cross sections.

### Acknowledgements

I thank my colleagues from H1 and ZEUS for their work reflected in this contribution.

### REFERENCES

1. ZEUS Coll., M. Derrick *et al.*, *Phys. Lett.* **B 315** (1993) 481; H1 Coll., T. Ahmed *et al.*, *Nucl. Phys.* **B 429** (1994) 477.
2. J. Collins, *Phys. Rev.* **D 57** (1998) 3051, *err.-ibid.* **D 61** (2000) 19902.
3. H1 Coll., paper 981 subm. to ICHEP 2002.
4. H1 Coll., paper 980 subm. to ICHEP 2002.
5. H1 Coll., C. Adloff *et al.*, *Z. Phys.* **C 76** (1997) 613.
6. H1 Coll., paper 984 subm. to ICHEP 2002.
7. ZEUS Coll., paper 821 subm. to ICHEP 2002.

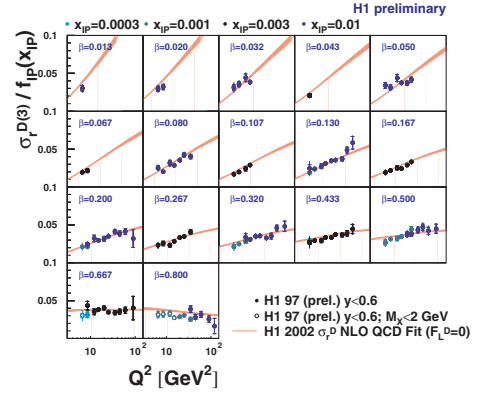


Figure 9.  $Q^2$  dependence of  $\sigma_r^D$  from H1, scaled by  $f_P(x_P)^{-1}$  and compared with the NLO QCD fit.

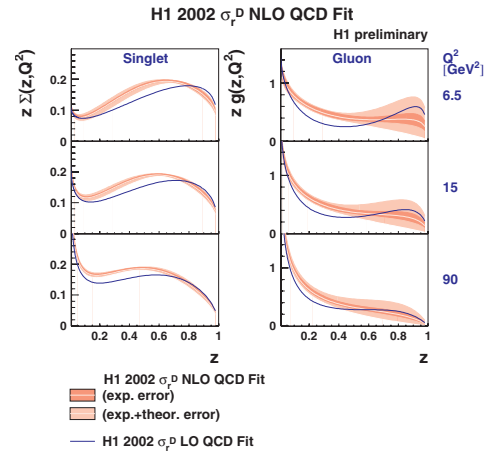


Figure 10. Diffractive singlet (left) and gluon (right) distributions from the H1 NLO QCD fit.

8. ZEUS Coll., J. Breitweg *et al.*, *Eur. Phys. J.* **C 6** (1999) 43.
9. ZEUS Coll., paper 822 subm. to ICHEP 2002.
10. J. Bartels, J. Ellis, H. Kowalski, M. Wüsthoff, *Eur. Phys. J.* **C 7** (1999) 443.
11. ZEUS Coll., paper 823 subm. to ICHEP 2002.
12. A. Savin, these proceedings.